

LETTERS

HP1- β mobilization promotes chromatin changes that initiate the DNA damage response

Nabieh Ayoub¹, Anand D. Jeyasekharan¹, Juan A. Bernal¹ & Ashok R. Venkitaraman¹

Minutes after DNA damage, the variant histone H2AX is phosphorylated by protein kinases of the phosphoinositide kinase family, including ATM, ATR or DNA-PK¹. Phosphorylated (γ -H2AX)—which recruits molecules that sense or signal the presence of DNA breaks, activating the response that leads to repair^{2,3}—is the earliest known marker of chromosomal DNA breakage. Here we identify a dynamic change in chromatin that promotes H2AX phosphorylation in mammalian cells. DNA breaks swiftly mobilize heterochromatin protein 1 (HP1)- β (also called CBX1), a chromatin factor bound to histone H3 methylated on lysine 9 (H3K9me). Local changes in histone-tail modifications are not apparent. Instead, phosphorylation of HP1- β on amino acid Thr 51 accompanies mobilization, releasing HP1- β from chromatin by disrupting hydrogen bonds that fold its chromodomain around H3K9me. Inhibition of casein kinase 2 (CK2), an enzyme implicated in DNA damage sensing and repair^{4–6}, suppresses Thr 51 phosphorylation and HP1- β mobilization in living cells. CK2 inhibition, or a constitutively chromatin-bound HP1- β mutant, diminishes H2AX phosphorylation. Our findings reveal an unrecognized signalling cascade that helps to initiate the DNA damage response, altering chromatin by modifying a histone-code mediator protein, HP1, but not the code itself.

We used an enhanced green fluorescent protein (EGFP)-HP1- β fusion protein^{7–9} to monitor changes in the dynamic behaviour of HP1- β after DNA breakage. In undamaged cells, fluorescence recovery after photobleaching (FRAP), using a range of laser-light intensities (Supplementary Fig. 1a–d), showed that EGFP-HP1- β exhibits distinct molecular mobilities in euchromatin compared with heterochromatin^{7,8}. Exposure of cells to ionizing radiation alters the dynamics of EGFP-HP1- β FRAP in a statistically significant manner (Fig. 1a). Recovery in both euchromatin and heterochromatin occurs more swiftly, as demonstrated by a change in the association constant, K , calculated from a single component exponential fit for the FRAP curves (Supplementary Fig. 1e). Similar changes are induced by the clastogenic drug etoposide (data not shown). Therefore, HP1- β mobilization is not solely a response to ionizing radiation.

EGFP-HP1- β mobilization after DNA damage in euchromatin, as well as heterochromatin, is evident using fluorescence loss in photobleaching (FLIP), which measures the exchange of fluorescent molecules between distinct regions within a cell (Supplementary Fig. 1f), and thus, their relative diffusional mobility, provided that imaging and bleaching parameters are held constant¹⁰. The changes in FLIP dynamics of EGFP-HP1- β after exposure to ionizing radiation are equivalent in euchromatin and heterochromatin, with the best-fit

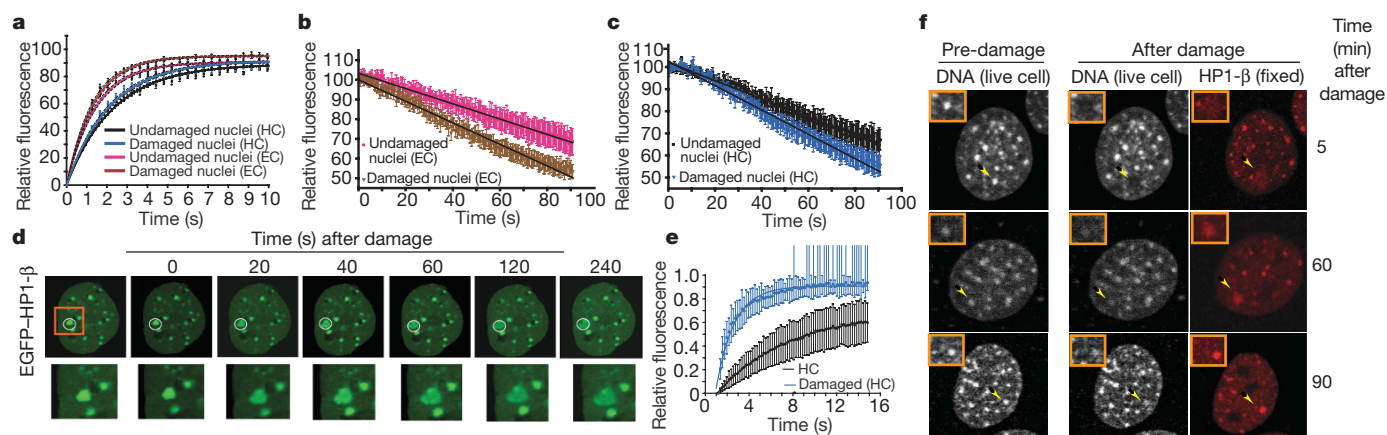


Figure 1 | Alterations in HP1- β dynamics and localization accompany its mobilization after DNA damage. **a**, Representation of the FRAP recovery curves ($n = 7$) of EGFP-HP1- β in euchromatin/nucleoplasm (EC) or heterochromatin (HC), before and after DNA damage by 10 Gy ionizing radiation, fitted (solid lines) to a single component exponential (dotted lines show 95% confidence intervals). Relative fluorescence intensity is plotted (y axis) against time (x axis). **b**, **c**, FLIP decay curves ($n = 7$) for euchromatin and heterochromatin before and after DNA damage, defining the acceleration in mobility of the EGFP-HP1- β protein after damage. The solid lines represent a single order polynomial fit of the data. **d**, Changes in the abundance and distribution of EGFP-HP1- β immediately after the

induction of laser-induced DNA damage in a single heterochromatin focus (white circle). The area bounded by the orange square is enlarged below each panel. **e**, FRAP curves for EGFP-HP1- β in heterochromatin before and after DNA damage ($n = 10$). **f**, Changes in endogenous HP1- β at defined time points (rows) after the induction of DNA damage to a heterochromatin focus. Hoechst staining of a live cell immediately before, and after, laser damage is shown in the first two columns. The third column shows the same cell after fixation and immunostaining for HP1- β . The area marked by the yellow arrow has been enlarged at the upper left corner of each frame. All results are typical of >3 independent experiments. Where shown, error bars represent s.e.m.

¹The Medical Research Council Cancer Cell Unit, Hutchison/MRC Research Centre, Hills Road, Cambridge CB2 0XZ, UK.

decay constant increasing from 0.4 ± 0.01 (s.e.m.) to 0.55 ± 0.01 in each ($P < 0.05$, $n = 7$, t -test), confirming exchange between the two compartments and suggesting that a similar mechanism causes mobilization in both (Fig. 1b, c).

We precisely targeted DNA double-strand breaks (DSBs), marked by γ -H2AX formation and 53BP1 recruitment, to specific living cells

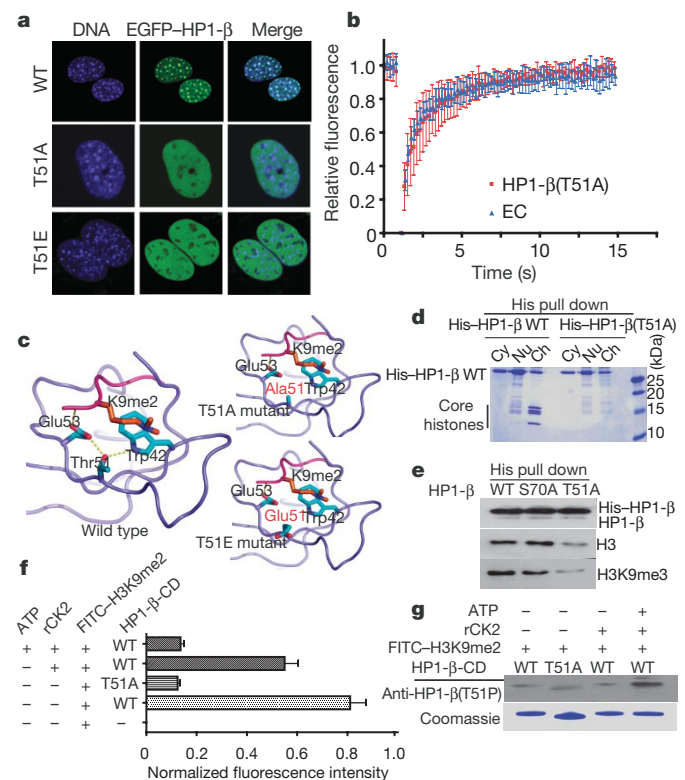


Figure 2 | Thr 51 substitution or phosphorylation alter the localization and dynamics of HP1- β by disrupting a hydrogen-bond network essential for the HP1-H3K9me interaction. **a**, Localization of wild-type (WT) EGFP-HP1- β (top panel) or mutant forms in which Thr 51 in the chromodomain has been replaced with alanine (T51A, middle panel) or glutamic acid (T51E, bottom panel). **b**, The dynamic behaviour of EGFP-HP1- β (T51A) measured by FRAP is similar to the high mobility of EGFP-HP1- β in euchromatin regions. Fluorescence recovery (relative fluorescence intensity, y axis) after photobleaching is shown over time ($n = 10$). Error bars represent s.d. **c**, A model for the interaction of the wild-type human HP1- β chromodomain bound to methylated K9 of histone H3 (K9me2), based on the PDB coordinates 1KNA, compared with its T51A and T51E mutants. A network of hydrogen bonds between the side chains of Glu 53, Thr 51 and Trp 42 of the human HP1- β chromodomain, marked as yellow dashed lines, is disrupted in the T51A and T51E mutants. **d**, Cytoplasmic (Cy), nuclear soluble (Nu) or chromatin-bound (Ch) proteins pulled down with His-tagged HP1- β wild-type or T51A mutant proteins in a Coomassie-stained 12% SDS-PAGE gel. The identity of the four core histones, pulled down by the wild-type but not the T51A mutant protein, was confirmed by mass spectrometry (data not shown). **e**, Western blot analysis of proteins pulled down with His-tagged HP1- β wild-type, S70A or T51A mutant proteins in nuclear extracts. Blots were probed with antibodies against HP1- β (top row), histone H3 (middle row) or histone H3K9me3 (bottom row). The S70A mutant, whose localization and dispersal after DNA damage are indistinguishable from the wild-type protein, serves as a control. All three variants equally pull down endogenous HP1- β . **f**, **g**, Interaction of the HP1- β chromodomain with methylated H3K9 is disrupted by CK2 phosphorylation on Thr 51. **f**, Fluorescence intensities (x axis) of a fixed volume of glutathione beads used to pull down a FITC-H3K9me2 peptide incubated with the different GST-HP1- β chromodomain fusion proteins listed ($n = 3$, error bars represent s.e.m.). Decreased peptide binding (that is, fluorescence intensity) occurs when the GST-HP1- β chromodomain is phosphorylated on Thr 51, as demonstrated in **g** by probing protein eluted from the glutathione beads with anti-HP1- β (T51P). Equal loading of GST-HP1- β chromodomain in each track is shown by Coomassie staining.

or discrete regions within a single nucleus (Supplementary Fig. 2a–c), using a 405-nm laser¹¹. Damage to a single heterochromatin focus (Fig. 1d, circled white) swiftly disperses EGFP-HP1- β , inciting local rearrangement and spreading within 20 s (Fig. 1d and Supplementary Movies 1 and 2), but with little overall variation in DNA staining (Supplementary Fig. 2d), distinct from reported changes in GFP-tagged histone H2B¹². The FRAP dynamics of EGFP-HP1- β changes locally at damage sites (Fig. 1e). Endogenous HP1- β visualized by immunofluorescence is also rearranged and dispersed from a damaged heterochromatin focus within 5 min after DNA damage, to re-accumulate gradually over 90 min (Fig. 1f), consistent with a physiological response to DNA breakage and repair.

HP1- β localizes to chromatin via its direct interaction with H3K9me (Supplementary Fig. 3a). Unexpectedly, neither the distribution nor abundance of H3K9me3 staining is altered after DNA damage. This is also true for trimethylation of histone H3 on lysine 4 (H3K4me3) (Supplementary Fig. 3b), and acetylation of histone H3 on lysines 14 or 18 (ref. 13) or acetylation of histone H4 on lysine 16 (Supplementary Fig. 3c). Thus, it seems unlikely that alterations in the histone code mobilize HP1- β after DNA damage. Instead, mobilization may result from changes in HP1- β itself, akin to previous reports^{14,15}.

Substitution of eight putative phosphorylation sites in HP1- β affected neither the localization nor the damage-induced dispersal of EGFP-HP1- β from heterochromatic foci (Supplementary Fig. 4). By contrast, alteration of Thr 51 in the HP1- β chromodomain either to Ala or to Glu (respectively expected to preclude, or mimic, phosphorylation) suffices to distribute mutant EGFP-HP1- β diffusely throughout the nucleus (Fig. 2a) and to confer rapid dynamics in FRAP (Fig. 2b). Similarly, replacement of the corresponding residue, Thr 50, in human HP1- α (Supplementary Fig. 5a) excludes HP1- α from heterochromatin (Supplementary Fig. 5b).

Thr 51 is evolutionarily conserved (Supplementary Fig. 6a). The structure of the HP1- β chromodomain (Fig. 2c), modelled from a *Drosophila melanogaster* HP1-H3K9me complex¹⁶, reveals that the hydroxyl moiety in the Thr 51 side chain participates in a hydrogen-bond network essential for complex formation. Phosphorylation or replacement of Thr 51 is expected to disrupt this hydrogen-bond network (Fig. 2c), diminishing the capacity of HP1- β to bind to chromatin via H3K9me3. Indeed, whereas His-tagged HP1- β (His-HP1- β) effectively pulls down the four core histones from cell extracts (Fig. 2d), mutant His-HP1- β (T51A) does not. Moreover, His-HP1- β and its Ser70Ala mutant both bind efficiently to histone H3K9me3 from chromatin, although mutant His-HP1- β (T51A) does not (Fig. 2e). Thus, Thr 51 modification suffices to release HP1- β from chromatin, although additional, DNA-damage-induced changes could also assist.

In human HP1- β , Thr 51 lies within an atypical phospho-acceptor site for CK2 (Supplementary Fig. 6b)¹⁷, divergent from the consensus Ser/Thr-X-X-Asp/Glu. Indeed, recombinant (r) CK2 can phosphorylate the wild-type HP1- β chromodomain (but not its T51A mutant form), confirming that this residue is a specific target (Supplementary Fig. 6c–e). An antibody specific to the phosphopeptide SDEDN(pThr)WEPEEC reacts *in vitro* with recombinant HP1- β wild-type protein solely after exposure to rCK2, but not with the T51A mutant (Supplementary Fig. 6f). *In vivo*, the antibody reacts with the wild-type but not the mutant protein (Supplementary Fig. 7a). This reactivity increases after etoposide-induced DNA damage, with kinetics parallel to γ -H2AX formation.

Phosphorylation of the HP1 chromodomain on Thr 51 by rCK2 releases it from binding to a fluorescein-tagged H3K9me2 peptide (Fig. 2f). The fluorescent peptide is pulled down by the HP1 chromodomain, but not by its T51A mutant. Thr 51 phosphorylation by rCK2 (Fig. 2g) diminishes binding of the fluorescent H3K9me2 peptide to background levels.

In cells treated with isoform-specific short interfering (si)RNAs targeting HP1- β , diminished HP1- β expression corresponds with

diminished anti-HP1- β (T51P) staining after etoposide-induced DNA damage (Fig. 3a, b). Ionizing radiation also elicits an increase in anti-HP1- β (T51P) staining, which is inhibited by pre-incubation with the phosphopeptide immunogen (Supplementary Fig. 7b). There is increased nucleoplasmic and local staining for HP1- β (T51P) specifically in damaged nuclei marked by γ -H2AX phosphorylation, and not in undamaged ones, after laser irradiation at 405 nm (Fig. 3c) or 365 nm (Supplementary Fig. 7c). Laser damage to a heterochromatin focus triggers dispersal of endogenous HP1- β accompanied by spreading HP1- β (T51P) staining around the damaged region (Fig. 3d). Together, these findings suggest that HP1- β (T51P) is created locally in damaged chromatin and thereafter released, mirroring the pattern of HP1- β rearrangement and dispersal.

Inhibition of CK2 activity by chemical or genetic means suppresses damage-induced changes in HP1- β dynamics and its phosphorylation on Thr 51. In cell extracts, anti-HP1- β (T51P) detects a species

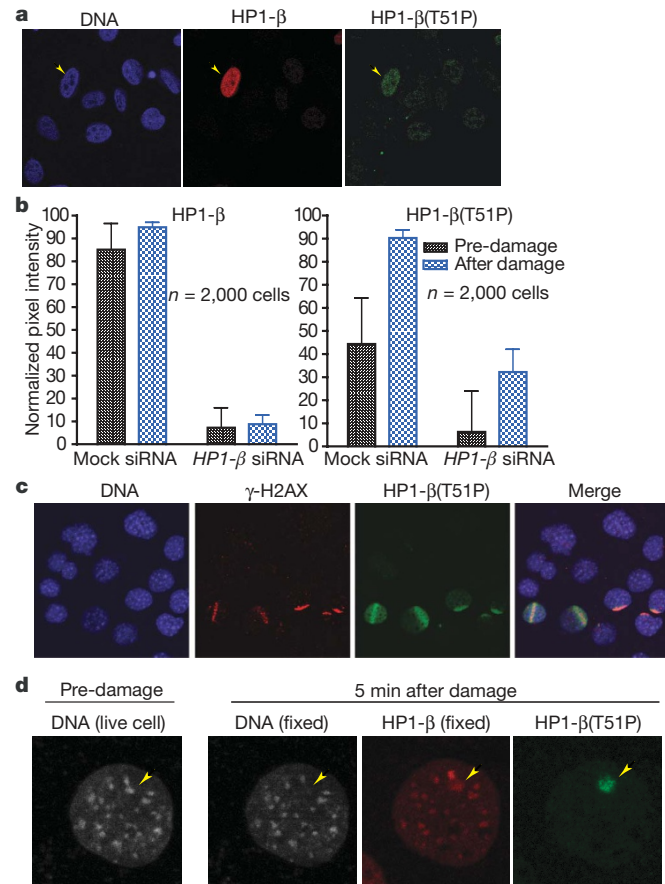


Figure 3 | Thr 51 phosphorylation is induced after DNA damage and accompanies HP1- β dispersal from damage sites. **a**, U2OS cells treated 72 h after HP1- β depletion with 20 μ M etoposide for 1 h before fixation. Nuclei (DNA in blue) were stained with anti-HP1- β (red) and anti-HP1- β (T51P) (green). HP1- β (T51P) staining is visible only in cells spared from HP1- β depletion (yellow arrow). **b**, Immunofluorescence intensity per cell for HP1- β (left) and HP1- β (T51P) (right) after HP1- β knockdown and etoposide treatment ($n = 2,000$, error bars represent s.d.) measured with a Cellomics HCS microscope. Both the induction of anti-HP1- β (T51P) staining after DNA damage in the mock siRNA control as well as a significant decrease of average HP1- β (T51P) staining intensity per cell after HP1- β depletion are evident. **c**, Representative field of mouse embryonic fibroblasts (MEFs) damaged by 405-nm laser micro-irradiation fixed and stained within 5 min after damage. HP1- β (T51P) staining (green) is present only in damaged nuclei (DNA in blue) marked by γ -H2AX formation (red). **d**, Localized induction of anti-HP1- β (T51P) (green) accompanying HP1- β dispersal (red) in a single 405-nm laser-damaged heterochromatin focus (yellow arrow). The first panel is a live cell image of Hoechst staining before radiation showing the undamaged heterochromatin focus.

684

with mobility corresponding to HP1 (Supplementary Fig. 7d), enhanced in a dose-dependent manner by etoposide treatment. Chemical inhibition of CK2 with 4,5,6,7-tetrabromo-benzimidazole (TBB) at 75 μ M for 6 h, a concentration required to suppress CK2 activity in living cells¹⁸, diminishes both the background detection and etoposide-induced enhancement of HP1- β (T51P) levels (Supplementary Fig. 7b, d). Genetic suppression of CK2 activity by an overexpressed dominant-negative form of the enzyme¹⁹ is enough to suppress Thr 51 phosphorylation after DNA damage (Fig. 4a, b). Finally, in living cells TBB suppresses the changes in FRAP dynamics (Fig. 4c) usually triggered by DNA damage. Together, these observations demonstrate that CK2 mediates the mobilization of HP1- β from chromatin after DNA breakage via Thr 51 phosphorylation.

Chromatin alterations may accompany phosphoinositide kinase activation^{20,21} or modulate γ -H2AX deposition along chromosomes^{12,22,23}, but whether they help to trigger the response to DNA breaks is unknown. We not only find that CK2 inhibition suffices to diminish histone H2AX phosphorylation after DNA breakage

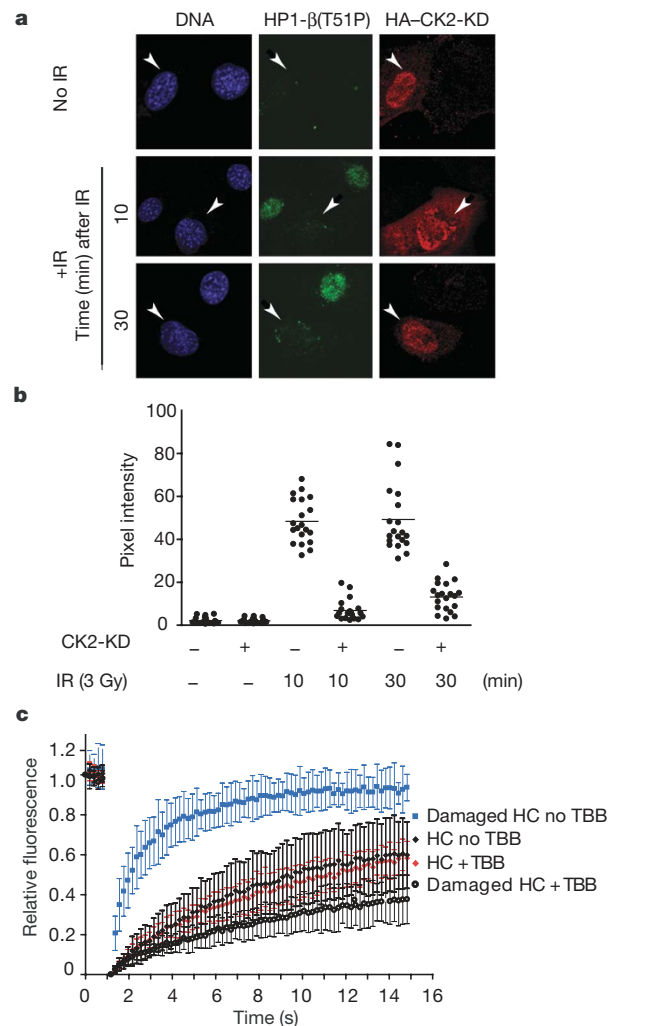


Figure 4 | Inhibition of CK2 suppresses the phosphorylation of HP1- β on Thr 51 and mobilization after DNA damage. **a**, MEFs (nuclei in blue) transfected with a haemagglutinin (HA)-epitope-tagged, kinase-dead (KD) K69M CK2 α' mutant. Anti-HA staining in red marks the transfected cells, whereas anti-HP1- β (T51P) staining is in green. Transfected cells (arrowheads) have less HP1- β (T51P) staining after 3 Gy ionizing radiation (IR) compared to neighbouring, untransfected cells. **b**, Quantitative representation of anti-HP1- β (T51P) staining intensity per cell under the specified experimental conditions ($n = 30$, $P < 0.05$ by analysis of variance (ANOVA)/Dunnett's post test). **c**, The dynamic behaviour of EGFP-HP1- β after DNA damage, with (black circles) or without (blue squares) pre-exposure to 75 μ M of the CK2 inhibitor TBB.

(Fig. 5a, b and Supplementary Fig. 8a, b), but also that immobilization of HP1- β on chromatin suppresses γ -H2AX formation. We fused EGFP-HP1- β to the histone H2B in a strategy previously used to render proteins constitutively chromatin-bound¹⁰ whether before or after DNA damage (Supplementary Fig. 9). The intensity of γ -H2AX staining after DNA damage is inhibited in cells expressing the immobilized H2B-EGFP-HP1- β fusion protein (Fig. 5c, d). Neither EGFP-HP1- β nor H2B-EGFP (Fig. 5c, d) expression to similar levels affects γ -H2AX staining, ruling out that this effect is merely the result of HP1- β overexpression or high levels of chromatin-bound H2B. Instead, our findings collectively show that mobilization of HP1- β from chromatin facilitates H2AX phosphorylation after DNA damage. We propose on this basis that dynamic alterations in chromatin structure triggered by HP1- β mobilization promote H2AX phosphorylation, so far the earliest known event in the response to chromosomal breakage.

How CK2 can be activated locally within seconds at damage sites is not understood. Intriguingly, although neither HP1- β nor CK2 seems to be a direct substrate of phosphoinositide-kinase-family kinases²⁴, chemical inhibition of these enzymes decreases but does not prevent HP1- β phosphorylation (Supplementary Fig. 10),

suggestive of crosstalk with the damage-activated CK2 signalling cascade.

Notably, HP1- β mobilization after DNA damage provides an unusual example of a mechanism that alters chromatin organization by targeting a histone-binding protein, rather than the histone code itself²⁵. Such a mechanism could facilitate both the rapid remodelling of chromatin after DNA damage, as well as its efficient reversal by HP1- β dephosphorylation.

METHODS SUMMARY

Transfection. We used established protocols for Lipofectamine 2000 (Invitrogen).

Microscopy and laser-induced DNA damage. DNA damage by laser-irradiation was by pre-sensitization with Hoescht 33342, followed by exposure to a 405-nm diode laser, or a pulsed 365-nm micropoint laser beam. DNA breakage was confirmed using staining for γ -H2AX and 53BP1. Dispersal of EGFP-tagged proteins was followed by live-cell sequential imaging every 0.3 s. Alternatively, dispersed proteins were detected by fixation and immunostaining. Dynamic exchange was studied by photobleaching EGFP-tagged proteins, and measuring fluorescence recovery in the bleached area (FRAP), or its loss from a distant area during repetitive bleach cycles (FLIP). All imaging of EGFP-tagged proteins was with an argon 488 laser line (attenuated to 1%) on a Zeiss LSM 510-META Confocor2. Average per-cell fluorescence intensity measurements were analysed with the Zeiss LSM software, from images acquired using identical acquisition parameters. Where indicated, immunofluorescence experiments were performed in 96-well plates and analysed using a Cellomics HCS automated microscope and associated software.

Biochemical assays. His-, glutathione S-transferase (GST)-, or antibody-mediated pull downs were performed using modifications of standard methods. Binding of a fluorescent methylated Lys 9 (K9me) peptide to GST-HP1 was quantified on a Fusion plate-reader.

Western blotting. Modifications to standard methods are described in the Methods section. Signal intensities were quantified by integrated density measurements on ImageJ software.

Statistical analysis. This was performed using GraphPad Prism 4.0.

Full Methods and any associated references are available in the online version of the paper at www.nature.com/nature.

Received 14 November 2007; accepted 28 February 2008.

Published online 27 April 2008.

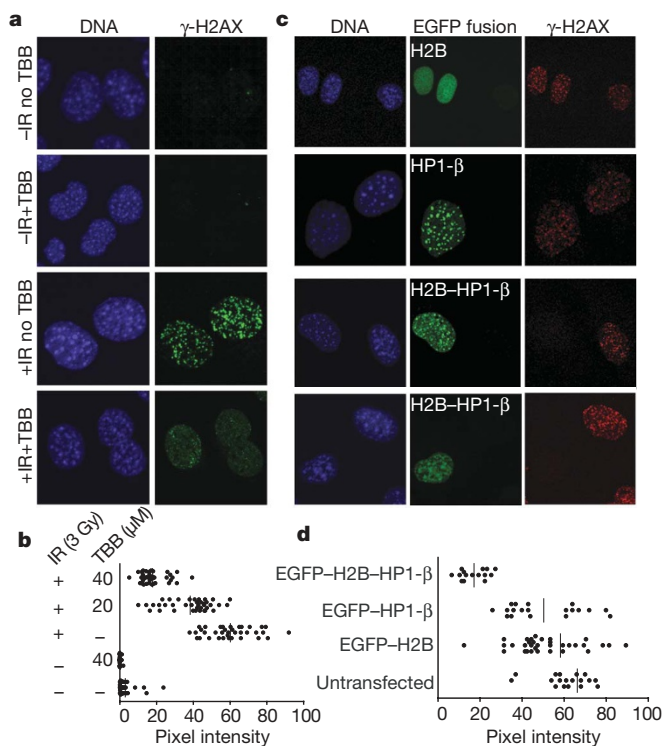


Figure 5 | HP1- β mobilization by CK2 promotes H2AX phosphorylation.

a, Pre-exposure of MEFs to 75 μ M TBB suppresses γ -H2AX foci formation at 5 min after 3 Gy ionizing radiation. DNA is stained blue; γ -H2AX is green. The top two rows show undamaged cells without (-IR no TBB) or with (-IR + TBB) pre-exposure; the bottom two rows represent ionizing-radiation-damaged cells without (+IR no TBB) or with TBB pre-exposure (+IR + TBB). **b**, Dot-plot showing that the pixel intensity of γ -H2AX staining after damage under identical imaging conditions is reduced in a dose-dependent manner by TBB pre-exposure ($n = 20$ per sample, $P < 0.01$, independent t -tests). **c**, An H2B-EGFP-HP1- β fusion protein constitutively immobilized on chromatin suppresses γ -H2AX foci formation at 5 min after 3 Gy ionizing radiation. DNA is stained blue, the different EGFP fusion proteins are stained green, and γ -H2AX is red. The top two rows show MEFs transfected with constructs encoding EGFP-HP1- β or H2B-EGFP, whereas the bottom two rows both show H2B-EGFP-HP1- β . Untransfected cells within the same field provide an internal control. **d**, Dot-plot representing the pixel intensities of γ -H2AX signal per cell under identical imaging conditions for cells with and without the transfected constructs ($n = 20$, $P < 0.05$ with t -test/ANOVA for multi-group comparison).

- Rogakou, E. P., Pilch, D. R., Orr, A. H., Ivanova, V. S. & Bonner, W. M. DNA double-stranded breaks induce histone H2AX phosphorylation on serine 139. *J. Biol. Chem.* **273**, 5858–5868 (1998).
- Fernandez-Capetillo, O., Lee, A., Nussenzweig, M. & Nussenzweig, A. H2AX: the histone guardian of the genome. *DNA Repair (Amst.)* **3**, 959–967 (2004).
- Lowndes, N. F. & Toh, G. W. DNA repair: the importance of phosphorylating histone H2AX. *Curr. Biol.* **15**, R99–R102 (2005).
- Allende-Vega, N., Dias, S., Milne, D. & Meek, D. Phosphorylation of the acidic domain of Mdm2 by protein kinase CK2. *Mol. Cell. Biochem.* **274**, 85–90 (2005).
- Cheung, W. L. *et al.* Phosphorylation of histone H4 serine 1 during DNA damage requires casein kinase II in *S. cerevisiae*. *Curr. Biol.* **15**, 656–660 (2005).
- Loizou, J. I. *et al.* The protein kinase CK2 facilitates repair of chromosomal DNA single-strand breaks. *Cell* **117**, 17–28 (2004).
- Festenstein, R. *et al.* Modulation of heterochromatin protein 1 dynamics in primary mammalian cells. *Science* **299**, 719–721 (2003).
- Cheutin, T. *et al.* Maintenance of stable heterochromatin domains by dynamic HP1 binding. *Science* **299**, 721–725 (2003).
- Schmiedebeg, L., Weisshart, K., Diekmann, S., Meyer Zu Hoerster, G. & Hemmerich, P. High- and low-mobility populations of HP1 in heterochromatin of mammalian cells. *Mol. Biol. Cell* **15**, 2819–2833 (2004).
- Lukas, C., Falck, J., Bartkova, J., Bartek, J. & Lukas, J. Distinct spatiotemporal dynamics of mammalian checkpoint regulators induced by DNA damage. *Nature Cell Biol.* **5**, 255–260 (2003).
- Rogakou, E. P., Boon, C., Redon, C. & Bonner, W. M. Megabase chromatin domains involved in DNA double-strand breaks *in vivo*. *J. Cell Biol.* **146**, 905–916 (1999).
- Kruhlak, M. J. *et al.* Changes in chromatin structure and mobility in living cells at sites of DNA double-strand breaks. *J. Cell Biol.* **172**, 823–834 (2006).
- Kuo, M. H. *et al.* Transcription-linked acetylation by Gcn5p of histones H3 and H4 at specific lysines. *Nature* **383**, 269–272 (1996).
- Zhao, T. & Eisenberg, J. C. Phosphorylation of heterochromatin protein 1 by casein kinase II is required for efficient heterochromatin binding in *Drosophila*. *J. Biol. Chem.* **274**, 15095–15100 (1999).
- Zhao, T., Heyduk, T. & Eisenberg, J. C. Phosphorylation site mutations in heterochromatin protein 1 (HP1) reduce or eliminate silencing activity. *J. Biol. Chem.* **276**, 9512–9518 (2001).

16. Jacobs, S. A. & Khorasanizadeh, S. Structure of HP1 chromodomain bound to a lysine 9-methylated histone H3 tail. *Science* **295**, 2080–2083 (2002).
17. Formby, B. & Stern, R. Phosphorylation stabilizes alternatively spliced CD44 mRNA transcripts in breast cancer cells: inhibition by antisense complementary to casein kinase II mRNA. *Mol. Cell. Biochem.* **187**, 23–31 (1998).
18. Ruzzene, M., Penzo, D. & Pinna, L. A. Protein kinase CK2 inhibitor 4,5,6,7-tetrabromobenzotriazole (TBB) induces apoptosis and caspase-dependent degradation of haematopoietic lineage cell-specific protein 1 (HS1) in Jurkat cells. *Biochem. J.* **364**, 41–47 (2002).
19. Canton, D. A., Zhang, C. & Litchfield, D. W. Assembly of protein kinase CK2: investigation of complex formation between catalytic and regulatory subunits using a zinc-finger-deficient mutant of CK2 β . *Biochem. J.* **358**, 87–94 (2001).
20. Bakkenist, C. J. & Kastan, M. B. DNA damage activates ATM through intermolecular autophosphorylation and dimer dissociation. *Nature* **421**, 499–506 (2003).
21. Ziv, Y. *et al.* Chromatin relaxation in response to DNA double-strand breaks is modulated by a novel ATM- and KAP-1 dependent pathway. *Nature Cell Biol.* **8**, 870–876 (2006).
22. Kim, J.-A., Kruhlak, M., Dotiwala, F., Nussenzweig, A. & Haber, J. E. Heterochromatin is refractory to γ H2AX modification in yeast and mammals. *J. Cell Biol.* **178**, 209–218 (2007).
23. Cowell, I. G. *et al.* γ H2AX foci form preferentially in euchromatin after ionising radiation. *PLoS ONE* **2**, e1057 (2007).
24. Matsuoka, S. *et al.* ATM and ATR substrate analysis reveals extensive protein networks responsive to DNA damage. *Science* **316**, 1160–1166 (2007).
25. Lomberk, G., Bensi, D., Fernandez-Zapico, M. E. & Urrutia, R. Evidence for the existence of an HP1-mediated subcode within the histone code. *Nature Cell Biol.* **8**, 407–415 (2006).

Supplementary Information is linked to the online version of the paper at www.nature.com/nature.

Acknowledgements We thank L. Pellegrini for modelling the HP1–H3K9me2 structure; M. Daniels, S. Y. Peak-Chew, M. Lee, R. Kulkarni and P. Rowling for technical assistance; and T. Misteli, T. Jenuwein and D. Litchfield for gifts of material. N.A. acknowledges a fellowship from the International Agency for Research on Cancer, Lyon, France, J.A.B. a long-term fellowship from EMBO, Heidelberg, Germany, and A.D.J. a scholarship from the Gates Cambridge Trust. The UK Medical Research Council supports work in A.R.V.'s laboratory.

Author Contributions N.A. performed the experiments reported here, except that A.D.J. determined EGFP–HP1- β mobilization by FRAP and FLIP, demonstrated the release of Thr 51-phosphorylated HP1 from H3K9me, and performed the quantification of immunofluorescence, whereas J.A.B. helped to identify HP1- β phosphorylation sites, and measured the rCK2 kinetics. A.R.V. planned the project, helped to interpret the data and wrote the paper.

Author Information Reprints and permissions information is available at www.nature.com/reprints. Correspondence and requests for materials should be addressed to A.R.V. (arv22@cam.ac.uk).

METHODS

FRAP and FLIP assays. MEFs were seeded in 2-well Lab-Tek chambers (Nunc) after transfection with the EGFP-HP1- β construct. Before imaging, growth medium was replaced with phenol-red free L15 imaging medium. Live cell imaging and photobleaching experiments were performed using a $\times 40$ 1.2 NA water immersion lens on a Zeiss LSM 510 Meta confocal microscope (using a heating chamber to maintain the cells at 37 °C) with the 488-nm line of an argon laser operating at 6.1 A.

FRAP analysis was performed by a method previously established in our laboratory²⁶. For low-bleach FRAP (see Supplementary Fig. 1), selected regions of heterochromatin and euchromatin were simultaneously bleached in a diffraction-limited spot with a pulse of two iterations at 100% of the 15-mW 488-nm argon laser. Post-bleach images were acquired at a lower frequency of an image every 400 ms. Image bleach was corrected separately for euchromatin and heterochromatin regions using a nearby unbleached cell. For high-bleach FRAP experiments, photobleaching was carried out with 35 iterations at the same laser output, and images were collected every 290 ms. The normalized curves were plotted in GraphPad Prism, and recovery curves were fitted to a single order exponential equation $Y = Y_{\max}(1 - \exp(-KX))$ to yield a recovery constant K , shown to be different among groups by the sum of squares f -test at $P < 0.05$.

Transfected cells for analysis were chosen under epifluorescence. Transfection levels were controlled by using cells of similar nuclear size, that were visible but not saturated, at a fixed imaging intensity (1% transmission at maximal scan speed and fixed photomultiplier tube gain at an optical slice of 1.5 μm). An integrative time-bleach series was set up to take 5 initial images, then bleach a $2 \times 2 \mu\text{m}$ square with 30 iterations of 100% laser intensity in an euchromatin region every 4 images, for a total of 200 images. The cells were imaged with a fixed $\times 7$ zoom and fixed bleach region of interest (ROI) size in a 512×512 pixel image window to keep the time between images constant for different cells to allow comparison. Circular regions of heterochromatin and euchromatin of similar size (1- μm radius) equidistant at 10 μm from the site of bleaching were then chosen, and the pixel intensities during the FLIP procedure recorded. The procedure was performed on control and irradiated cells (10 min after ionizing radiation to allow temperature equilibration and decreased drift during scanning), with control cells also kept at room temperature for 20 min to compensate for the irradiation process. Nearby imaged—but unbleached—cells were used to correct for the effect of imaging during the FLIP procedure. For the data analysis, the raw pixel intensities were transferred into GraphPad Prism and converted into relative intensities as a percentage of the mean of the first three values. These intensities were plotted across time to generate the FLIP decay curves with standard errors being calculated from multiple measurements ($n = 7$, in repeated experiments, limited to avoid discrepancies from changes in time after irradiation). The curves were fit to a single order polynomial equation $y = a + bx$ and the decay constant b shown to be statistically different for different groups at $P < 0.05$ using the f -test.

Laser micro-irradiation. Laser micro-irradiation was used to induce DNA damage by modifying a previously described method²⁷. Briefly, cells were grown on chambered, 1-thickness borosilicate-glass cover slides (Nunc), incubated with $10 \mu\text{g ml}^{-1}$ Hoechst dye 33342 for 5 min at 37 °C, washed twice with Leibovitz's L-15 medium (Gibco), and further incubated in this medium. Cells were imaged using a Zeiss LSM 510 Meta inverted confocal microscope fitted with a heated stage unit for live-cell imaging (heating insert P, Zeiss). Heterochromatin or euchromatin regions, selected based on EGFP-HP1- β localization, were damaged by applying 200 iterations of 100% power from a 405-nm diode laser. To monitor changes, serial time-lapse images were taken at 256×256 pixel 8-bit resolution with a scan speed of 293 ms, using the 488-nm line from the argon laser at 1% power. For some experiments, cells were fixed at the indicated times for staining and immunofluorescence.

A pulsed N_2 laser system with a 365-nm dye cell (Micropoint; Photonics systems) coupled to the epifluorescence path of a Zeiss 510 LSM Confocor2 was also used for DNA damage experiments to induce localized damage in a large number of cells. The cycling time was set at approximately 10 Hz and the power used to excite Hoechst for DNA damage (calibrated by γ -H2AX staining)

was set at maximal attenuation of laser output through the supplied gradient neutral density filter (approximately 75%). Cells visualized under phase contrast were moved by manual operation of the motorized stage through a fixed point of laser illumination to induce stripes of DNA damage across several nuclei. Typically, 100–200 cells were damaged per experiment, and then fixed for immunofluorescence.

Immunofluorescence. Cell staining and immunofluorescence analyses were carried out as described previously². Briefly, transfected and untransfected cells were grown on coverslips and subjected to different treatments as indicated in the text before fixation. Cells were fixed using 4% formaldehyde for 10–15 min, followed by solubilization and blocking with 3% BSA in PBS, 0.05% Tween-20, 0.05% Triton. Imaging was performed on a Zeiss LSM 510 Meta confocal microscope, using a $\times 40$ objective with fixed optical slice, laser power and detector/amplifier settings for all samples across each individual experiment to allow comparison. Quantitative analysis for HP1- β (T51P) and γ -H2AX staining was performed using mean per-nucleus intensity to avoid any discrepancy in the definition or counting of foci. This was performed on identically stained and imaged samples by estimation of raw pixel intensity values for a defined number of cells, specified for each experiment, through the Zeiss LSM software, and comparison of the different groups by one-way ANOVA and Dunnett's post test. High-content microscopy was also used for certain experiments; 96-well plates (Nunc) with cells seeded at 3,000 per well were treated with specified DNA-damaging agents, pre-treatments/siRNA, then fixed and immunostained. The plates were imaged and analysed using a Cellomics high-content screening microscope, using a $\times 40$ non-immersion objective. Hoechst staining was used for object identification and the average intensity of fluorescent signal per nucleus was estimated using the target activation Cellomics bio-application. Five-hundred cells were analysed per well, and standard errors were calculated from an average of the means of eight wells.

Expression and purification of HP1- β . Full-length human HP1- β or its chromodomain were expressed in *Escherichia coli* BL21 (Stratagene) as carboxy-terminal fusions to GST using the pGEX4T3 vector (Pharmacia). Bacteria expressing the fusion protein were lysed in PBS supplemented with 5 mM dithiothreitol, 0.5% NP-40 and protease inhibitors, and the soluble fraction was applied onto glutathione-Sepharose 4B beads (Amersham). After extensive washing, full-length HP1- β and the chromodomain fragment were cleaved from the GST moiety using thrombin protease (Amersham) in PBS at 22 °C for 16 h. Thrombin was removed from the sample by chromatography with benzamidine-Sepharose 4B (Amersham).

Peptide synthesis and binding assay. A peptide (FITC-H3K9me2) encoding residues 1–15 of the H3 tail dimethylated on Lys 9 and amino-terminally labelled with fluorescein was synthesized by PeptideCrest Limited. Ten micrograms of purified GST-HP1 chromodomain (or its T51A mutant form), 3 nmol of FITC-H3K9me2 peptide (representing a tenfold molar excess over HP1) and 20 μl of 50% GST bead slurry were added to a PBS-based binding buffer containing 0.2% NP-40 and 0.1% BSA, and incubated at room temperature for 1 h. For phosphorylation experiments, 25 μl of a kinase reaction containing 10 μg GST-HP1 chromodomain protein, 5,000 units rCK2, in CK2 buffer containing 50 μM ATP, replaced the unmodified GST-HP1 chromodomain. After binding, the mixture was centrifuged at 5,000g for 3 min and all supernatant removed by gentle aspiration. The beads were re-suspended in 50 μl binding buffer, transferred to assigned wells of a 96-well plate, and fluorescence intensity read using a Fusion microplate reader (PerkinElmer). A mixture of FITC-H3K9me2 and beads alone was used to calibrate background binding, to which the rest of the data were normalized before export to GraphPad Prism to calculate mean intensities and standard errors from different runs ($n = 3$). Changes in binding were shown to be significant using a student's t -test.

26. Daniels, M. J., Marson, A. & Venkataraman, A. R. PML bodies control the nuclear dynamics and function of the CHFR mitotic checkpoint protein. *Nature Struct. Mol. Biol.* 11, 1114–1121 (2004).
27. Rogakou, E. P., Boon, C., Redon, C. & Bonner, W. M. Megabase chromatin domains involved in DNA double-strand breaks *in vivo*. *J. Cell Biol.* 146, 905–916 (1999).